UC Merced

UC Merced Previously Published Works

Title

Developmental alterations in brain network asymmetry in 3- to 9-month infants with congenital sensorineural hearing loss

Permalink

https://escholarship.org/uc/item/6ft0b25j

Journal

Science Advances, 11(42)

ISSN

2375-2548

Authors

Liu, Guangfang
Zhou, Xin
Hu, Zhenyan
et al.

Publication Date

2025-10-17

DOI

10.1126/sciadv.adx1327

Copyright Information

This work is made available under the terms of a Creative Commons Attribution License, available at https://creativecommons.org/licenses/by/4.0/

Peer reviewed

eScholarship.org Powered by the California Digital Library
University of California

Check for updates

DEVELOPMENTAL NEUROSCIENCE

Developmental alterations in brain network asymmetry in 3- to 9-month infants with congenital sensorineural hearing loss

Guangfang Liu[1]†, Xin Zhou[2,3]†, Zhenyan Hu[1]†, Yidi Liu[2], Endi Huo[1], Heather Bortfeld[4], Qi Dong[1], Chunhui Chen[1], Haihong Liu[2]*‡, Haijing Niu[1]*‡

Copyright © 2025 The Authors, some rights reserved; exclusive licensee American Association for the Advancement of Science. No claim to original U.S. Government Works. Distributed under a Creative Commons Attribution NonCommercial License 4.0 (CC BY-NC).

Auditory exposure plays a crucial role in shaping brain development, but little is known about whether and how an initial lack of auditory exposure might disrupt the development of functional network lateralization. We addressed this issue by acquiring functional near-infrared spectroscopy data from infants aged 3 to 9 months with congenital sensorineural hearing loss (SNHL). The SNHL infants showed efficient small-world characteristics within each hemisphere. However, unlike typically developing controls, who showed an age-related leftward lateralization of network efficiencies, SNHL infants did not exhibit the emergence of hemispheric asymmetry. Intriguingly, lateralization of frontal efficiency was preserved in SNHL infants with mild hearing loss but declined significantly with increasing severity of hearing impairment. These findings suggest that even SNHL infants with some residual hearing experience disruption in the development of functional lateralization. This underscores the importance of providing early auditory access to SNHL infants to support robust functional integration during early development.

INTRODUCTION

Sensorineural hearing loss (SNHL) is the most prevalent congenital sensory deficit in neonates, affecting ~0.83 to 3.43% of newborns at birth (*1*–*3*). Infancy represents a critical period in neurodevelopment, marked by rapid changes in brain structure and function as infants engage with their environments (*4*, *5*). Disruptions in sensory input during this period, particularly in modalities that support cognitive, social, and linguistic development, can have lasting consequences for long-term outcomes (*6*, *7*).

One key developmental process that is sensitive to early sensory input is brain lateralization, the emergence of functional and structural asymmetries between the two cerebral hemispheres (*8*, *9*). These asymmetries reflect the brain's specialization for distinct yet integrated functions. The left hemisphere is typically dominant for language and motor control, whereas the right hemisphere is more engaged in spatial processing, face perception, and affective prosody (*9*, *10*). From infancy through childhood, functional lateralization is recognized as a hallmark of typical brain development (*11*, *12*).

Auditory experience plays a central role in the development of these lateralized networks (*13*, *14*). Neuroimaging evidence shows that hemispheric asymmetries in auditory processing begin to emerge within the first months of life. Early in development (e.g., in infants aged 2 to 12 months), the right hemisphere responds more robustly to auditory input, whereas the left hemisphere gradually becomes dominant for language-relevant processing (*15*, *16*). This leftward shift is paralleled by the emergence of asymmetries in functional network organization and has been observed in both infants (3 to 9 months) and older children (6 to 9 years) (*17*, *18*).

Reduced auditory input in infancy may alter or delay these normative developmental trajectories. In animal models, cochlear absence or limited auditory stimulation leads to changes in spatial mapping in the auditory cortex and dysregulation of plasticity-related signaling pathways (*19*, *20*). Human neuroimaging studies show that children with congenital SNHL exhibit increased connectivity within auditory network and salience network (*21*), reduced connectivity in the default mode network (*22*), diminished white matter integrity (e.g., superior longitudinal and inferior fronto-occipital fasciculi) (*23*), and lower spontaneous neural activity (*24*). These findings suggest that reduced auditory input may lead to widespread reorganization of structural and functional networks, potentially affecting hemispheric specialization.

It is important to distinguish between the effects of limited auditory input and the absence of early language exposure. Although SNHL restricts access to sound, it does not necessarily hinder language development. Infants who are exposed to a fully accessible signed language from birth, typically those with deaf signing parents, often develop typical patterns of brain asymmetry related to language, even in the absence of auditory input (*7*, *25*). In contrast, infants with SNHL who lack exposure to an accessible language, whether spoken or signed, during the early months of life may show more pronounced differences in brain organization (*19*). Increasing evidence suggests that having or not having access to language has a distinct and profound impact on both brain and behavioral development (*26*). These findings challenge the notion that auditory input alone drives hemispheric specialization and instead emphasize the crucial role of both sensory and linguistic experiences in shaping the developing brain.

The present study focuses specifically on infants with congenital SNHL who have not had early access to a fully accessible signed language. This group represents a critical but understudied population:

[1]State Key Laboratory of Cognitive Neuroscience and Learning & IDG/McGovern Institute for Brain Research, Beijing Normal University, Beijing 100875 China. [2]Department of Otolaryngology Head and Neck Surgery, Beijing Children's Hospital, Capital Medical University, National Center for Children's Health, Beijing 100045 China. [3]Department of Audiology and Vestibular Medicine, Senior Department of Otolaryngology Head and Neck Surgery, The Sixth Medical Center of PLA General Hospital, Chinese PLA Medical School, Beijing 100853 China. [4]Departments of Psychological Sciences and Cognitive and Information Sciences, University of California, Merced, Merced, CA, USA.
*Corresponding author. Email: niuhjing@bnu.edu.cn (H.N.); haihongliu6@aliyun.com (H.L.)
†These authors contributed equally to this work.
‡These authors contributed equally to this work.

Downloaded from https://www.science.org at University of California Merced on November 03, 2025

infants who experience auditory input loss alongside minimal early language exposure before any clinical intervention. Although previous studies have explored brain organization in children and adults with SNHL (*21*–*24*), the emergence of these neural differences during infancy remains poorly understood.

In this study, we investigated topological network asymmetries between the cerebral hemispheres in infants between 3 and 9 months of age with congenital SNHL and no early sign language exposure, compared to age-matched typically developing (TD) controls. We hypothesized that a lack of auditory input, coupled with delayed language exposure, would disrupt the typical development of hemispheric asymmetry in functional brain networks. Using resting-state functional near-infrared spectroscopy (fNIRS), we collected imaging data from 112 infants (52 SNHL and 60 TD). Hemispheric functional networks were constructed for each infant, and topological metrics of efficiency, which reflect the brain's capacity for integration and segregation, were extracted. We then examined developmental changes in these asymmetry measures across the two groups.

This study examines the early developmental trajectory of hemispheric network asymmetry in infants with SNHL and no early sign language input. These findings provide insight into how sensory and linguistic experiences shape early brain lateralization and have important implications for both theory and clinical practice. A better understanding of when and how these differences emerge can inform the timing and type of early interventions, including cochlear implantation (CI) and early language access.

RESULTS

Efficient small-world properties of the hemispheric networks for SNHL and TD infants

Small-world properties are crucial features of human brain networks, facilitating the efficient segregation of specialized information processing and the integration of information across regions. For each cortical hemisphere in both the SNHL and TD infants, we constructed functional connectivity networks and calculated their small-world attributes. Visually, the infants with SNHL showed widespread decreased functional connectivity within the left or right hemispheric network compared to TD infants (Fig. 1A); however, similar to the TD infants, the network organization in SNHL infants exhibited typical small-world properties. Specifically, the global efficiency of the left or right hemispheric networks in each group was nearly equivalent to that of their respective matched random networks, whereas the network local efficiency was larger than that of their matched random networks. These patterns led to the normalized global efficiency being approximately equal to 1 and the normalized local efficiency being greater than 1, which are the typical features of small-world topology (Fig. 1, B and C). The small-world organization indicates that brain network in both SNHL and TD infants is efficient for both global information transmission and local information processing.

Developmental changes in hemispheric asymmetry of global and local network efficiencies

Hemispheric asymmetry differences

Hemispheric asymmetry represents a fundamental organizing principle of the human brain and has been proposed as a marker of successful neurodevelopment. We therefore investigated hemispheric asymmetries in network efficiency metrics (e.g., global efficiency, E_{glob}; local efficiency, E_{loc}) during development in both TD and SNHL infants. The asymmetry index (AI) for global and local efficiency was calculated to examine age-related changes in both groups. For global efficiency, general linear model (GLM) analysis revealed significantly divergent developmental trajectories between groups, with a significant group × age interaction for hemispheric asymmetry ($t = 2.60$, $P = 0.011$). Post hoc analysis showed a significant developmental increase in hemispheric asymmetry for TD infants ($r = 0.31$, $P = 0.015$) but nonsignificant change for SNHL infants ($r = -0.16$, $P = 0.27$) (Fig. 2A). For local efficiency, a significant group × age interaction in hemispheric asymmetry was also found ($t = 2.19$, $P = 0.030$). Post hoc analysis showed a trend toward developmental increase in hemispheric asymmetry for TD infants ($r = 0.21$, $P = 0.099$) and a nonsignificant change for SNHL infants ($r = -0.19$, $P = 0.18$) (Fig. 2B).

Hemisphere effects

To further examine whether developmental differences in network efficiency varied by group or hemisphere, we reran GLM analysis including group (TD and SNHL), hemisphere (left and right), age (in months), and all two-way and three-way interactions. Significant group × hemisphere × age interaction effects were observed for both global efficiency [$F(1,102) = 8.59$, $P = 0.004$] and local efficiency [$F(1,102) = 6.36$, $P = 0.013$]. To clarify developmental differences in efficiency measures related to two-way interactions, we conducted separate GLM analyses for each group, including hemisphere, age, and the hemisphere × age interaction (Fig. 3, A and B). This analysis helps determine whether observed leftward lateralization results from accelerated development in the left hemisphere or delayed maturation in the right hemisphere. The results showed a significant hemisphere × age interaction effect on global efficiency [$t = 2.99$, $P = 0.009$; false discovery rate (FDR)–corrected] and a marginally significant interaction effect on local efficiency ($t = 2.24$, $P = 0.059$; FDR-corrected) in TD infants, whereas no significant results were observed in infants with congenital SNHL (E_{glob}: $t = -1.13$, $P = 0.26$; E_{loc}: $t = -1.44$, $P = 0.16$; FDR-corrected). Further analysis showed that the TD infants exhibited significant developmental increases in both global efficiency ($r = 0.35$, $P = 0.006$) and local efficiency ($r = 0.34$, $P = 0.008$) in the left hemisphere, whereas no significant developmental changes were observed in the right hemisphere for these two efficiency measures (E_{glob}: $r = 0.17$, $P = 0.19$; E_{loc}: $r = 0.20$, $P = 0.12$) (Fig. 3A). In SNHL infants, marginally significant developmental decreases were observed for both metrics in the left hemisphere (E_{glob}: $r = -0.24$, $P = 0.094$; E_{loc}: $r = -0.25$, $P = 0.072$) but not right hemispheres (E_{glob}: $r = -0.13$, $P = 0.37$; E_{loc}: $r = -0.14$, $P = 0.33$) (Fig. 3B). These results demonstrate that the disrupted development of network global and local efficiencies in the left hemisphere ultimately led to a developmental deficiency such that no leftward asymmetry emerged in infants with congenital SNHL.

Developmental changes in hemispheric asymmetry of regional nodal efficiency

Hemispheric asymmetry differences

Subsequently, we evaluated age-related changes in hemispheric asymmetry of mean nodal efficiency across frontal, temporal, parietal, and occipital regions in both TD and SNHL infants. A significant group × age interaction was observed only in the frontal region for hemispheric asymmetry of nodal efficiency ($t = 2.63$, $P = 0.039$; FDR-corrected). Post hoc analysis revealed a significant positive correlation between asymmetry and age in TD infants ($r = 0.35$, $P = 0.007$), whereas no such association was found in SNHL infants

Downloaded from https://www.science.org at University of California Merced on November 03, 2025

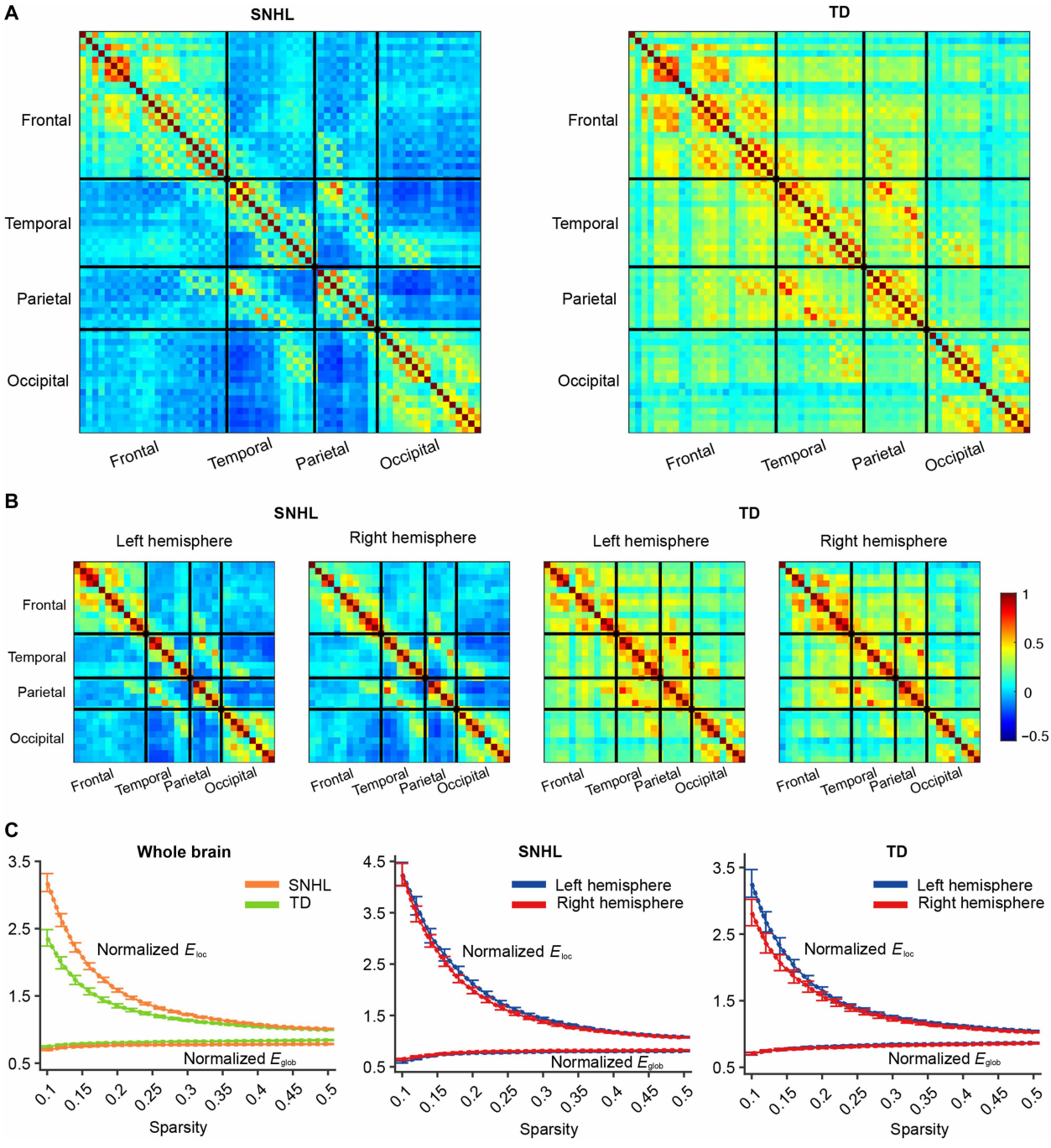


Fig. 1. Functional connectivity maps and small-world network characteristics of the functional networks in TD and congenital SNHL infants. (**A**) Whole-brain functional connectivity maps in SNHL and TD infants. (**B**) Functional connectivity maps of the left and right hemispheres in SNHL and TD. (**C**) Small-world properties of the functional networks. Error bars indicate the SEs of each subgroup.

($r = -0.12$, $P = 0.41$) (Fig. 4A). For the other cortical regions, no significant group × age interactions were found (temporal: $t = 1.09$, $P = 0.39$; parietal: $t = 1.06$, $P = 0.39$; occipital: $t = 0.81$, $P = 0.42$; FDR-corrected).

Hemisphere effects

For the frontal regions, we further investigated the group × hemisphere × age interaction effect on mean nodal efficiency and found a significant interaction effect [$F(1,103) = 8.23$, $P = 0.005$] for mean nodal efficiencies. To further clarify this three-way interaction, separate GLM analysis was conducted for each group, including hemisphere, age, and their interaction.

In TD infants, a significant hemisphere × age interaction was observed ($t = 3.12$, $P = 0.006$; FDR-corrected), with post hoc analysis showing a significant developmental increase in left-hemisphere nodal efficiency ($r = 0.37$, $P = 0.003$) but no change in the right hemisphere ($r = 0.12$, $P = 0.34$) (Fig. 4A). In SNHL infants, no

Downloaded from https://www.science.org at University of California Merced on November 03, 2025

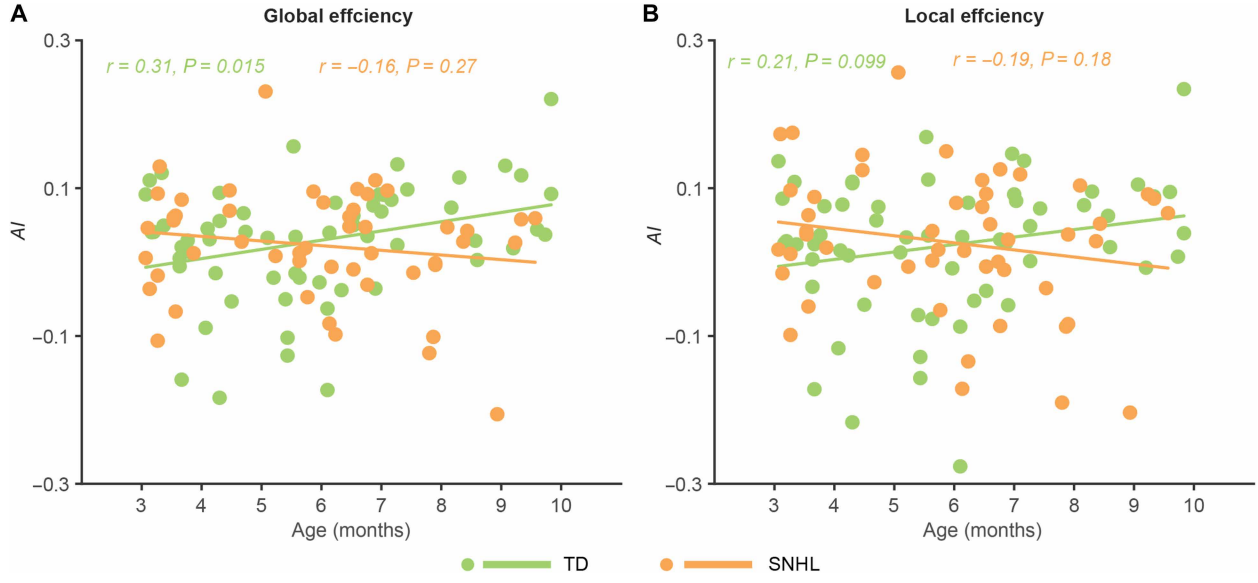


Fig. 2. Developmental differences in hemispheric networks for TD and congenital SNHL infants. (**A**) Developmental comparisons in the AI of global efficiency (E_{glob}). (**B**) Developmental comparisons in the AI of local efficiency (E_{loc}).

significant interaction was identified ($t = -0.79$, $P = 0.44$; FDR-corrected). Neither hemisphere showed developmental changes in nodal efficiency (left: $r = -0.22$, $P = 0.12$; right: $r = -0.17$, $P = 0.24$) (Fig. 4B).

Subgroup analysis of SNHL infants: impact of hearing loss severity on network lateralization

To investigate how the severity of hearing loss influences brain network lateralization, we categorized infants with SNHL into three groups on the basis of hearing loss severity: mild ($n = 20$), moderate-to-severe ($n = 15$), and profound ($n = 15$) groups. A GLM analysis was then conducted, including severity, hemisphere (left/right), and their interaction (severity × hemisphere) as factors, with brain network efficiency metrics as the outcome variables.

Global and local efficiencies

For global efficiency, a marginally significant severity × hemisphere interaction was observed [$F(2,47) = 2.83$, $P = 0.069$], whereas local efficiency showed no significant interaction [$F(2,47) = 1.80$, $P = 0.18$]. Post hoc analysis indicated that infants with mild hearing loss exhibited significantly higher global efficiency in the left hemisphere compared to the right ($t = 3.15$, $P = 0.003$; FDR-corrected), whereas no hemispheric differences were found in the moderate-to-severe ($t = -0.41$, $P = 0.68$; FDR-corrected) or profound groups ($t = 1.16$, $P = 0.25$; FDR-corrected) (Fig. 5A).

Frontal region analysis

In frontal regions, a significant severity × hemisphere interaction was observed [$F(2,47) = 3.31$, $P = 0.045$). Infants with mild hearing loss showed significantly higher nodal efficiency in the left frontal region compared to the right ($t = 4.31$, $P < 0.001$), whereas no hemispheric differences were found in the moderate-to-severe ($t = 1.21$, $P = 0.23$) or profound groups ($t = 0.59$, $P = 0.56$; FDR-corrected) (Fig. 5B).

Correlational analyses

Correlation analyses were conducted to examine the relationship between brain network metrics and hearing loss severity. Results showed that, as hearing impairment increased [indexed by higher auditory brainstem response (ABR) thresholds], nodal efficiency asymmetry in the frontal regions significantly decreased, indicating reduced leftward lateralization ($r = -0.31$, $P = 0.032$). No significant correlations were found between hearing loss severity and other efficiency measures or asymmetry indices (all $P > 0.05$) (Fig. 5C).

DISCUSSION

The present study examined the developmental changes in functional network asymmetries in 3- to 9-month-old infants with congenital SNHL, compared to age-matched TD controls. Results indicated that infants with SNHL preserved efficient small-world network properties within each hemisphere; however, they experienced the disruption of typical development in hemispheric asymmetries of functional network efficiency. Notably, left-hemisphere dominance in frontal nodal efficiency was preserved in infants with mild SNHL but declined significantly with increasing severity of hearing loss. These findings suggest that early auditory loss disrupts the normative trajectory of functional lateralization. Our results highlight the importance of early auditory intervention to support typical network specialization and reduce compensatory right-hemisphere recruitment in infants with SNHL.

Economic small-world characteristics of the hemispheric network in SNHL infants

Small-worldness is a fundamental property of human brain networks, characterized by an optimized organizational structure that supports both efficient information segregation and integration while minimizing wiring costs (*27*, *28*). Prior research has shown that small-world organization emerges in typically hearing infants as early as 3 months of age, and this efficient network architecture supports information processing across developmental stages, including in infancy (*17*), childhood (*18*), and adulthood (*18*, *29*). In contrast, disruptions to this efficient organization have been observed in various neurological disorders, including autism spectrum disorder (*30*), Parkinson's disease (*31*), and Alzheimer's disease (*32*).

Downloaded from https://www.science.org at University of California Merced on November 03, 2025

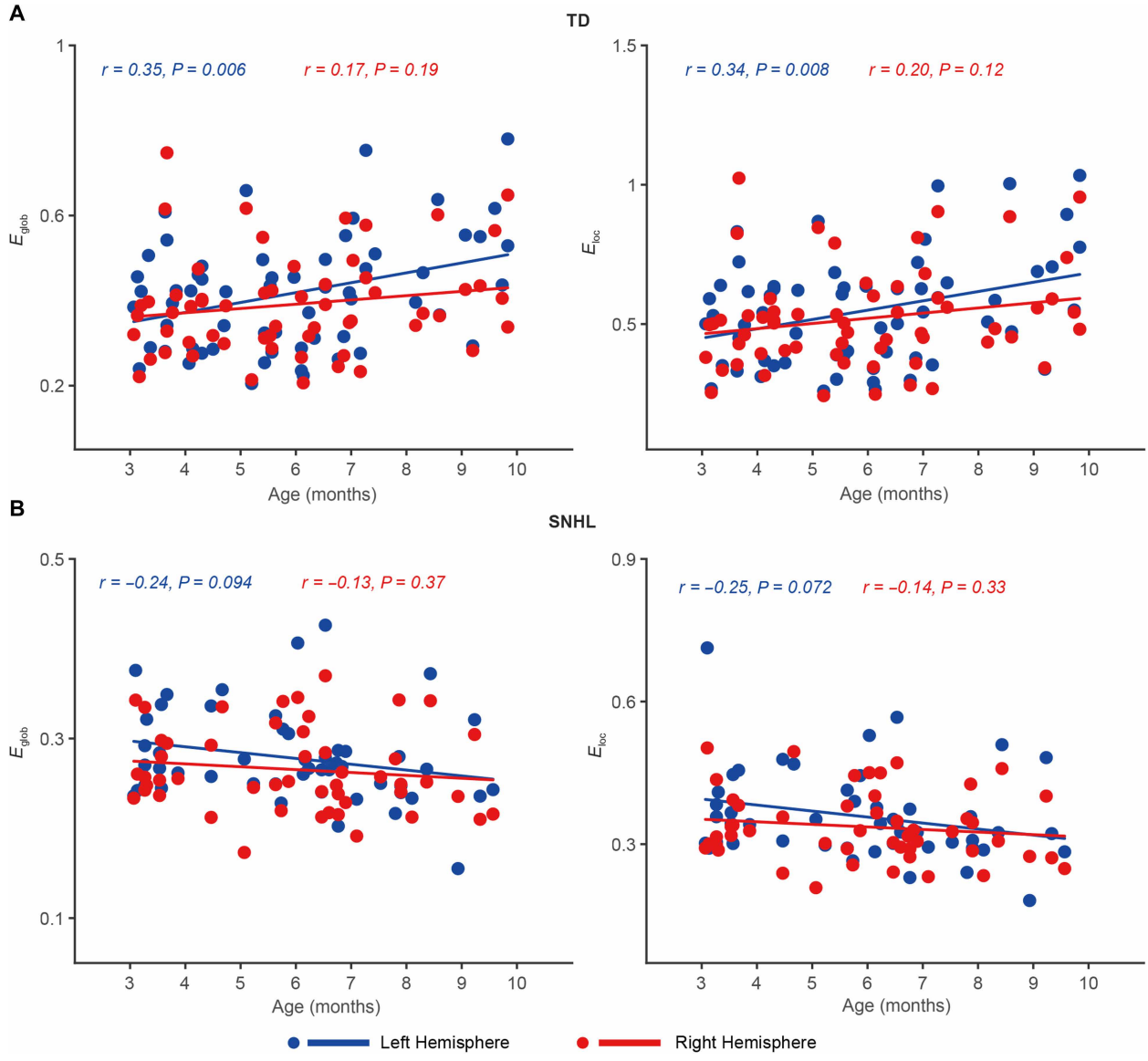


Fig. 3. Developmental differences in global efficiency (E_{glob}) and local efficiency (E_{loc}). (**A**) Developmental comparisons in E_{glob} and E_{loc} between the left and right hemispheres for TD infants. (**B**) Developmental comparisons in E_{glob} and E_{loc} between the left and right hemispheres for SNHL infants.

In infants with variable degrees of congenital hearing loss, we found that the small-world properties within each hemispheric network were preserved. This pattern is consistent with findings in TD infants, as well as with a prior study in children and adults with SNHL (*33*). Together, these results demonstrate that the core organizational architecture of brain networks remains intact in individuals who experience hearing loss, even early in life. This preservation provides a foundation for better understanding the broader impact of congenital SNHL on early brain development. Moreover, the findings highlight the brain's plasticity and resilience during critical periods of development, despite significant sensory loss.

Aberrant developmental trajectory of hemispheric network asymmetry in SNHL infants

How congenital hearing loss influences the early development of brain networks that are typically lateralized—a core organizational feature of the human brain—remains a critical and unresolved question. Hemispheric asymmetry, particularly in networks supporting auditory and language processing, emerges early in infancy (*17*, *34*) and continues to mature throughout childhood and adolescence (*18*, *35*), reflecting the brain's increasing specialization and efficiency. Age-related disruptions in hemispheric asymmetry have been observed in both adolescents and adults with early hearing loss (*36*), but the specific nature of these abnormalities remains unclear. For instance, Twomey *et al.* (*37*) reported atypical asymmetry patterns in individuals with congenital hearing loss, which varied depending on task modality. In contrast, Payne *et al.* (*38*) found that school-age children with congenital hearing loss (ages 5 to 8) still exhibited leftward hemispheric asymmetry during language production. These inconsistencies may largely be attributed to variations in participants' auditory exposure, language experience, or related cognitive abilities (*24*). Critically, the infants in this study had minimal auditory

Downloaded from https://www.science.org at University of California Merced on November 03, 2025

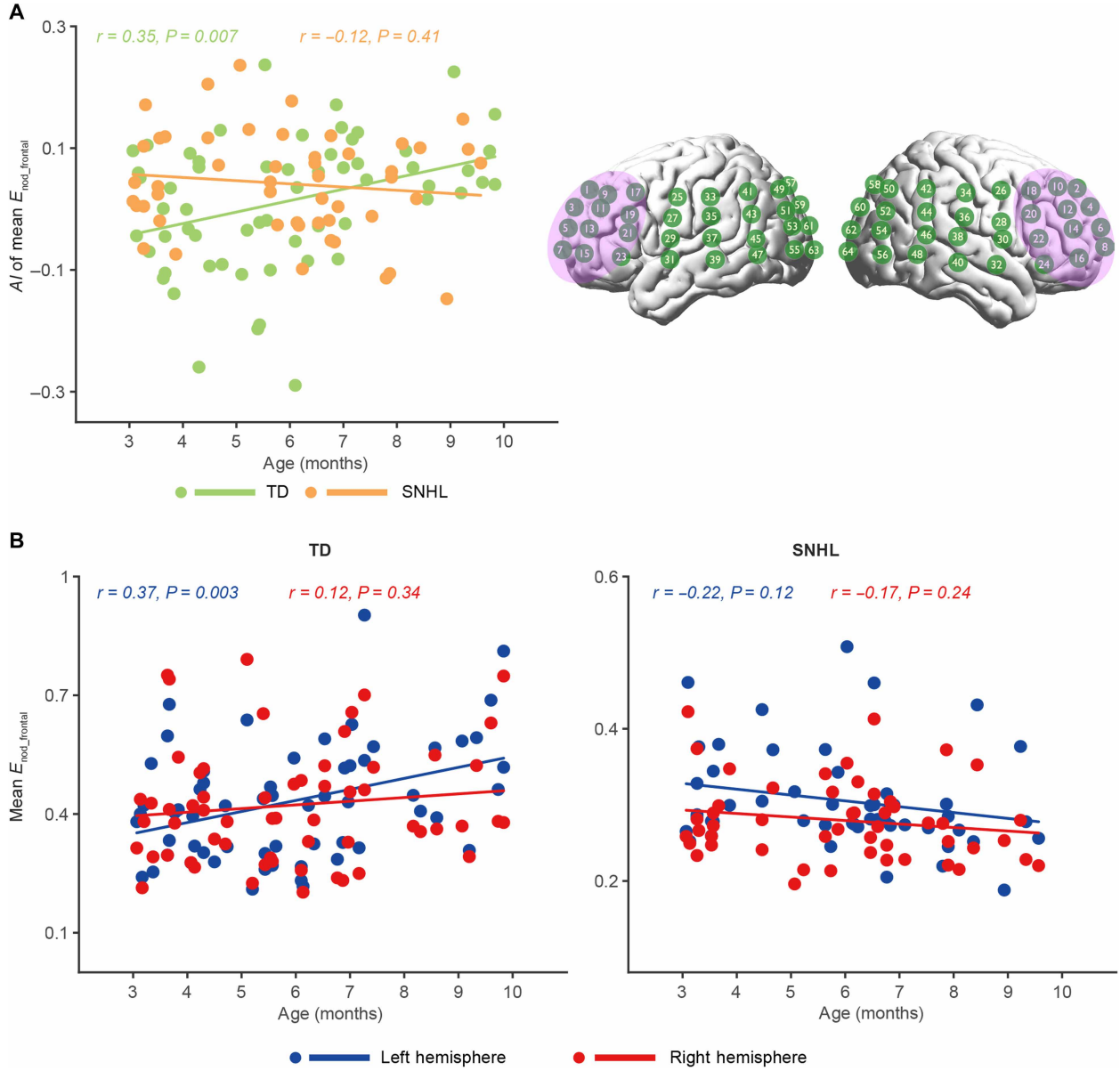


Fig. 4. Developmental differences in regional nodal efficiency for TD and congenital SNHL infants. (**A**) Developmental comparisons in the AI of frontal nodal efficiency. (**B**) Developmental comparisons in frontal nodal efficiency between the left and right hemispheres in TD and SNHL, respectively.

and language experience, suggesting that our findings reflect general brain developmental responses to early auditory input, rather than the more variable outcomes observed in older individuals with diverse language and communication histories.

In the current study, we observed that TD infants showed age-related increases in leftward network efficiency asymmetry across the first year of life, whereas infants with SNHL did not. Specifically, SNHL infants exhibited atypical development of hemispheric network asymmetry in frontal regions. Neurodevelopmentally, lateralized brain functions emerge through learning-dependent asymmetrical interactions between the two hemispheres (*39*). Without auditory input to support these maturational mechanisms, functional differentiation between the hemispheres may be delayed or even permanently altered. Critical aspects of functional brain network development (i.e., functional reorganization, cerebral lateralization, and cortical activation) likely occur early in life, particularly in visual, auditory, and sensorimotor regions, as sensory input markedly increases from the prenatal to postnatal period (*40*, *41*). Some auditory cortical responses in infants resemble those seen in adults, suggesting that, early in life, the brain already represents not only basic acoustic features (e.g., frequency, pitch, envelope) but also more complex, adult-like auditory characteristics (*42*). Whether these early cortical responses reflect inherent-innate-processing capacities or are shaped by early auditory experience remains an open question. However, our finding that leftward hemispheric asymmetry is disrupted in infants with congenital SNHL supports an experience-dependent account. Furthermore, given the relatively high metabolic activity of functional cortical areas in early infancy, these regions may be especially

Downloaded from https://www.science.org at University of California Merced on November 03, 2025

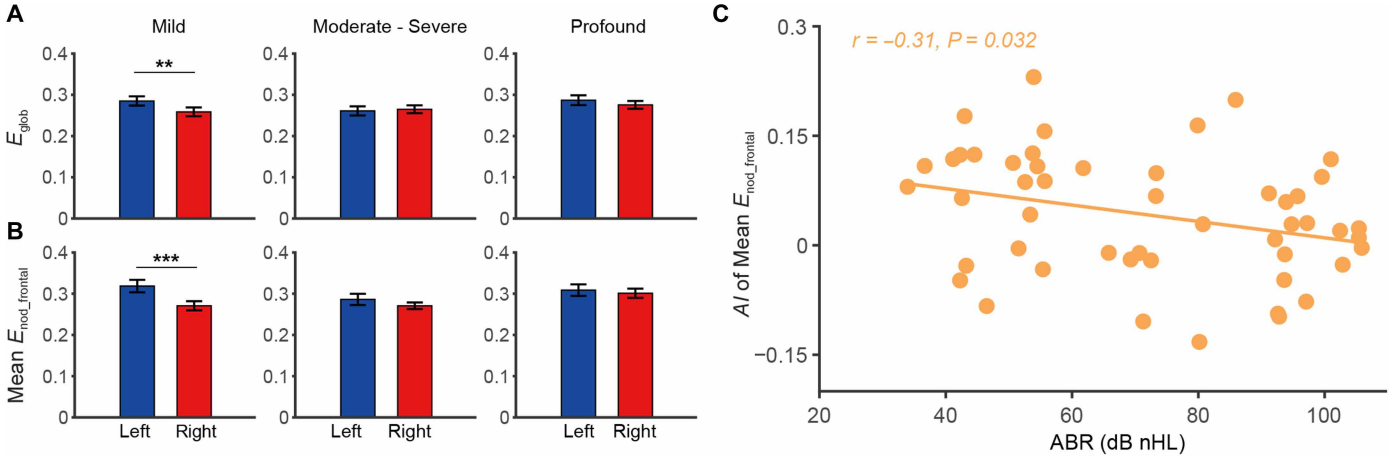


Fig. 5. Impact of hearing loss severity on network lateralization for SNHL infants. (**A**) Hemispheric differences in E_{glob} for infants with different hearing loss severity. Error bars indicate the SEs of each subgroup. (**B**) Hemispheric differences in frontal nodal efficiency for infants with different hearing loss severity. Error bars indicate the SEs of each subgroup. (**C**) Correlation between the ABR and AI of frontal nodal efficiency. $^{**}P < 0.01$ and $^{***}P < 0.001$.

vulnerable to atypical environmental influence, such as reduced auditory input, leading to altered developmental trajectories. Together, these findings point to a critical developmental window for the emergence of cerebral asymmetry, during which adequate auditory input is essential to support the typical leftward lateralization of brain networks.

Furthermore, the consequences of this altered developmental trajectory extend beyond neural architecture and are evident in behavioral outcomes. Longitudinal studies have shown that early hemispheric asymmetries, particularly in left auditory and frontal regions, predict later expressive and receptive language skills (*43*, *44*). In contrast, infants with SNHL often exhibit reduced or absent lateralization in core language regions (*24*, *45*, *46*). However, the implications of these neural differences for subsequent language development remain poorly understood as systematic longitudinal research is lacking. The disruption of hemispheric asymmetry observed in this study may represent an early neural marker of risk for language delay, highlighting the critical need for timely and individualized interventions in infants with hearing loss.

Disrupted development of network efficiency properties in the left hemisphere in SNHL infants

By focusing on infants early in the developmental process, the current study offers a fine-grained view of the emergence of hemispheric differences. Our network efficiency analysis revealed an age-related increase in both global and local efficiency in the left hemisphere among TD infants. However, this developmental trend was markedly attenuated in infants with congenital SNHL, suggesting that auditory experience is crucial for the maturation of left-hemispheric network efficiency. These findings are consistent with studies in adults with congenital hearing loss, which report that congenital deafness leads to distinct and altered functional organization in the left and right auditory cortices (*37*).

At the regional level, we found that the mean nodal efficiency of the left frontal lobe increased with age in TD infants, whereas infants with congenital SNHL exhibited symmetrical patterns in the frontal cortex, suggesting a lack of expected leftward specialization. These findings indicate that limited auditory input in early life may disrupt the age-related maturation of left-hemisphere functions, which typically emerge earlier than those in the right hemisphere.

The present finding of disrupted developmental trajectories of network efficiency in the left hemisphere among SNHL infants indicates that early insufficient auditory input interferes with the maturation in brain regions critical for language processing. Previous studies have shown that the left hemisphere undergoes earlier and more rapid maturation in language-related areas (*41*, *47*), and its experience-dependent development during sensitive periods renders it particularly vulnerable to insufficient auditory input. Our study provides evidence that adequate auditory exposure is vital for this aspect of early brain development. This aligns with evidence that congenital hearing loss disrupts the development of inter-regional connectivity (*48*), which may result in delayed or atypical language acquisition. Furthermore, as efficient network organization supports rapid information transfer and integration (*49*), impaired growth in network efficiency could underlie the broader cognitive delays reported in SNHL populations. The difficulties SNHL infants experience in processing auditory information before intervention may contribute to persistent deficits in language and cognitive development, even after interventions such as CI are introduced (*50*). Future longitudinal studies incorporating detailed behavioral assessments are needed to determine whether early interventions can normalize these neural trajectories and mitigate their long-term developmental impacts.

Relationship between brain development and severity of hearing loss in early life

Loss of normal stimulation of sensory cortices has the potential to cause maturational abnormalities (*51*). Childhood hearing loss represents a relatively common disruption of auditory experience, wherein severity-dependent auditory input loss gradients yield differential neurobiological outcomes. Children with severe or profound hearing loss exhibit delayed and/or deviant auditory cortical responses, as evidenced by abundant research (*52*). Similarly, adolescents who experienced early childhood mild-to-moderate hearing loss show persistent functional changes in auditory neural processing, including delayed auditory evoked potentials (*53*).

Downloaded from https://www.science.org at University of California Merced on November 03, 2025

This study demonstrates a significant impact of hearing loss severity on the lateralization of brain networks in infants. Specifically, infants with mild hearing loss exhibited typical leftward lateralization across the whole brain and within frontal regions, with both global efficiency (Fig. 5A) and frontal nodal efficiency (Fig. 5B) significantly higher in the left hemisphere compared to the right. In contrast, no significant hemispheric differences were observed in infants with moderate-to-severe or profound hearing loss. These findings suggest that, as the severity of hearing loss increases, the typical pattern of left-lateralization in brain networks progressively diminishes and disappears altogether. In normally hearing individuals, language-related regions, particularly in the temporal and frontal lobes, typically exhibit left-lateralization, which underpins efficient language processing and cognitive development (*54*). Correlational analyses (Fig. 5C) further supported this trend, revealing that higher ABR thresholds were associated with reduced lateralization in frontal nodal efficiency, reflecting a disruption of typical leftward specialization.

Of note, we did not observe age-related changes in the AI of global or local network efficiencies in infants with congenital SNHL, suggesting that early auditory input loss may underlie atypical patterns of cortical functional development. This finding aligns with previous research on children who experienced prolonged unilateral CI use before receiving bilateral CIs as these children also exhibited disrupted patterns of network asymmetry (*55*). Notably, another study has reported typical left-hemisphere dominance for language in both normally hearing children and those who received early access to CIs (*13*), highlighting the critical importance of early intervention in supporting the normative development of brain function in infants with SNHL.

Limitations

Although this study reveals significant developmental differences in hemispheric asymmetries of brain network efficiency, as well as a severity-dependent decline in lateralization among infants with SNHL, several limitations should be acknowledged.

First, the cross-sectional design limits our ability to examine individual developmental trajectories. Longitudinal studies are necessary to determine whether the observed disruptions in cerebral lateralization persist, worsen, or resolve over time, thereby providing stronger insights into neural plasticity and causal mechanisms. Second, although ABR testing was conducted during natural sleep to optimize recording conditions, subtle variations in infant arousal states may have introduced variability in wave V thresholds. Incorporating simultaneous electroencephalography (EEG) monitoring in future studies could help control for such state-dependent effects. Third, although neurodevelopmental screening excluded overt neurological abnormalities during infancy, it may not detect conditions such as autism spectrum disorder, attention-deficit/hyperactivity disorder, or language and intellectual delays. Extending follow-up periods and including comprehensive diagnostic assessments would improve our understanding of the long-term neurodevelopmental impact of SNHL. Fourth, although ABR testing was conducted during natural sleep to optimize recording conditions, infant arousal states could still vary subtly during testing, potentially introducing variability in wave V thresholds. As such, the correlation analyses between ABR thresholds and brain network metrics might be influenced by this physiological variability, particularly in younger infants where state control is less consistent. Future studies incorporating simultaneous EEG monitoring during ABR recordings could help better account for these state-dependent effects. Last, this study relied exclusively on fNIRS data; integrating additional neuroimaging modalities [e.g., magnetic resonance imaging (MRI) and EEG] and behavioral measures could offer a more holistic view of brain development in infants with SNHL.

MATERIALS AND METHODS

Participants

Table 1 provides a summary overview of the participant's demographic characteristics. Fifty-two congenital SNHL infants aged 3 to 9 months and 60 age- and gender-matched TD infants participated in this study. All infants in the study were full term, born after 37 weeks of pregnancy. Potential developmental abnormalities were excluded by neurodevelopmental screening and risk factors for hearing loss screening at 1 month of age. The screening materials used in the study were the 20-item Infant Neurological Motor Assessment (INMA) (*56*) and risk factors for early childhood hearing loss published by the Joint Committee on Infant Hearing (JCIH) (*57*), respectively. Congenital SNHL infants were all recruited from Beijing Children's Hospital, Capital Medical University, and none had received hearing loss intervention before this study. Of the TD infants, 20 were recruited from Beijing Normal University, whereas the remaining 40 were recruited from Beijing Children's Hospital, Capital Medical University. All participants were recruited following the same procedure. Informed consent was obtained from infants'

Table 1. Demographic characteristics of the SNHL and TD infants. Note: Data are presented as means ± SD. The *P* value was obtained using a two-tailed two-sample *t* test.

Characteristics	SNHL infants (*N* = 52)	TD infants (*N* = 60)	*P* value
Gender (male/female)	34/18	40/20	0.89
Age (months)	5.87 ± 1.89	5.91 ± 1.97	0.91
Head circumference (cm)	42.86 ± 1.95	42.83 ± 1.89	0.98
Degree of hearing loss			
Mild (30 < ABR ≤ 50 dB nHL)	22	–	–
Moderate (50 < ABR ≤ 70 dB nHL)	6	–	–
Severe (70 < ABR ≤ 90 dB nHL)	9	–	–
Profound (ABR > 90 dB nHL)	15	–	–

Downloaded from https://www.science.org at University of California Merced on November 03, 2025

parents, with experimental protocols (no. 2020-k-69) approved by the Institutional Review Board of Beijing Children's Hospital, Capital Medical University and the Institutional Review Board of State Key Laboratory of Cognitive Neuroscience and Learning, Beijing Normal University.

All infants received a full audiological diagnosis guided by the cross-check principle. The diagnosis test battery included ABR, auditory steady-state response (ASSR), distortion product otoacoustic emission (DPOAE), and acoustic impedance. These tests were performed during natural sleep induced by a sleep-withholding protocol, during which infants are deprived of sleep for ~4 hours before testing. Inclusion criteria for the congenital SNHL infant group were as follows: (i) bilateral thresholds of ABR Wave V > 30 dB normal hearing level (nHL); (iii) the average threshold of ASSR > 30 dB nHL at 0.5, 1, 2, and 4 kHz; (iii) bilateral 1-kHz tympanograms were single peaked, and 0.226-kHz tympanograms were type A; and (iv) bilateral DPOAE was absent at least four frequencies. (v) The difference in ABR hearing thresholds between ears was less than 20 dB. The mean and SD of hearing threshold differences between the two ears were 4.62 ± 6.27 dB. The statistical analysis showed that there had not significant difference between the hearing thresholds of the two ears ($z = -0.13$, $P = 0.90$, Wilcoxon signed-rank test), indicating symmetric hearing loss in SNHL infants in this study. Furthermore, inclusion criteria for the TD infants from Beijing Children's Hospital were as follows: (i) bilateral thresholds of ABR Wave V ≤ 30 dB nHL; (ii) an average threshold of ASSR ≤ 30 dB nHL at 0.5, 1, 2, and 4 kHz; (iii) bilateral 1-kHz tympanograms were single peaked, and 0.226-kHz tympanograms were type A; and (iv) bilateral DPOAE was present in at least four frequencies. Infants had no other known cognitive or neurological impairments, developmental delay, or active external or middle ear infections.

NIRS data recording

A continuous wave near-infrared optical imaging instrument (NirSmart, Hui Chuang, China) with a sampling rate of 10 Hz was used to measure hemodynamic changes in the cerebral cortex of the infants. Oxygenated hemoglobin (HbO) and deoxygenated hemoglobin (HbR) have different absorption spectra in the near-infrared wavelength region. The NIRS instrument exploits these optical properties of hemoglobin by using two wavelengths of light, 760 and 850 nm, which are differentially absorbed by the two chromophores. The probe array was composed of 24 sources and 16 detectors interlacing at the nearest distance of 3 cm, generating a total of 64 measurement channels covering the frontal, temporal, parietal, and occipital areas of each hemisphere (Fig. 6).

The experiment was conducted in a soundproof chamber with background noise < 20 dB(A). The probe array was symmetrically positioned on the infants' scalp following the 10-20 system, with reference to the external auditory canals, inion, and vertex as landmarks. Infants were held by their mothers during data collection, and mothers were instructed to remain silent and minimize movements during data acquisition to prevent displacement of the probes. For each infant, fNIRS data were collected for ~11 min while the infant was asleep.

MRI coregistration

To validate the position of the probes on the scalp, a structural MRI (sMRI) scan was acquired from a 6-month-old infant wearing probe arrays with vitamin E capsules. Vitamin E locations from these MRI scans were used as landmarks for coregistration, a common way to localize fNIRS probes relative to the brain (*58*, *59*). The scan was performed at the Imaging Centre in the Beijing Children's Hospital using a 3T Siemens Tim Trio MRI scanner. T1-weighted structural images were acquired using a magnetization-prepared rapid gradient echo (MPRAGE) sequence. The scanning parameters were as follows: slices = 152, TR = 6.67 ms, TE = 3.02 ms, FOV (field of view) = 202 mm by 202 mm, voxel size = 1 mm by 1 mm by 1 mm, flip angle = 8°, and slice orientation = sagittal. The sMRI data were normalized into Montreal Neurological Institute (MNI) space using a 6-month-old infant's brain template, and location coordinates were projected on the brain surface using NIRS-SPM software (http://bispl.weebly.com/nirs-spm.html) (*60*). The channels covered the frontal, temporal, parietal, and occipital areas of each hemisphere according to the automated anatomical labeling (AAL) template (*61*) (Fig. 6B).

Data preprocessing

Quality control

Similar to our previous study (*17*), we also used the in-house FC-NIRS package (*62*) (https://nitrc.org/projects/fcnirs) to preprocess

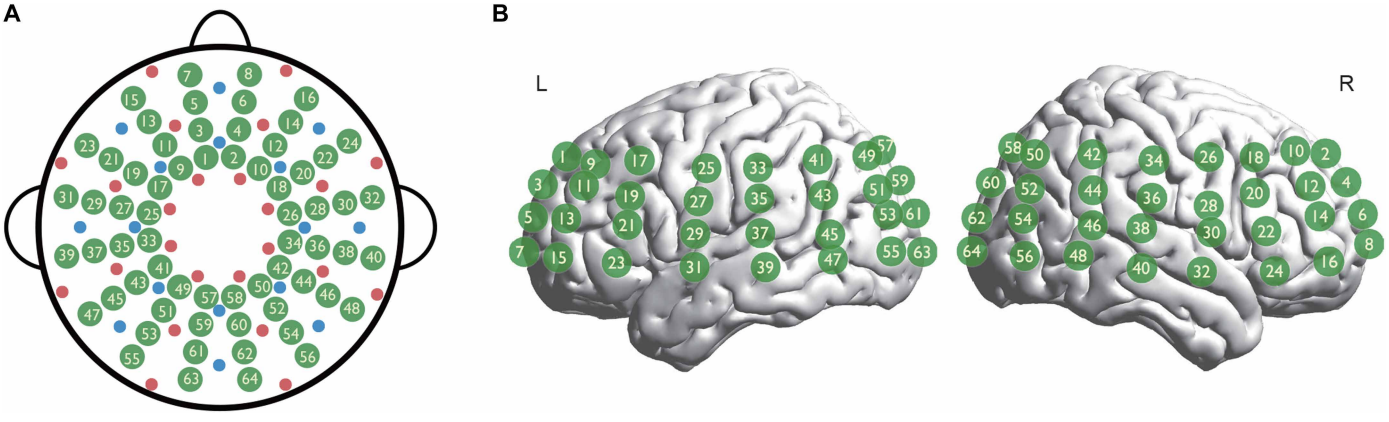


Fig. 6. fNIRS probe arrangement and MRI neuroanatomical coregistration. (**A**) Arrangement of the 64 measurement channels. The red and blue dots represent the sources and detectors, respectively. The green dots with digits represent the positions of the measurement channels. (**B**) MRI coregistration was conducted by an infant aged 6 months old wearing probe arrays with vitamin E capsules in MRI. Green dots with digits represent the measurement channels covering each hemisphere's frontal, temporal, parietal, and occipital areas.

Downloaded from https://www.science.org at University of California Merced on November 03, 2025

fNIRS data in this study. First, we examined the signal quality for each participant using three different approaches: signal-to-noise ratio (SNR), between-channel signal correlation, and frequency spectrum analysis. Generally, a measurement signal with low SNR was considered to be a "bad channel" reflecting poor contact between the optodes and scalp. Such bad channels are usually characterized by a low correlation between this signal and other signals, as assessed using signal correlation analysis. They also generally lack a cardiac component in the frequency spectrum analysis. We implemented these criteria as the basis for the removal of bad channels with poor signal quality from each participant. Participants with too many poor channels or the identified poor channels concentrated in a single hemisphere would be removed from further analysis. The number of removed bad channels ranged from 0 to 5 with a mean of 0.82 for SNHL infants and from 0 to 4 with a mean of 0.60 for TD infants, and no participant with poor channels concentrated in a single hemisphere was found. There did not show a significant difference on the number of removed channels between groups (t test, $P > 0.05$).

Reducing motion artifacts and global interference

Next, we detected and corrected motion-induced artifacts using the spline interpolation method (*63*). This approach calculates the moving standard deviation (MSD) within sliding windows of 2-s lengths. MSD values larger than 5 SDs from the mean were considered artifacts. The time series representing motion artifacts were further modeled via a cubic spline interpolation and subtracted from the original time series. Subsequently, we extracted a relatively stable time series from the processed data for each participant. If the duration of stable time series was much shorter, e.g., with a length of 2 to 3 min, across most measurement channels, the participant was excluded owing to insufficient reproducibility for calculating network efficiency metrics on the basis of a previous study (*64*). Two participants were excluded from further analysis. Of note, the number of time points corrected in this study was 406 for SNHL infants and 399 for TD infants, which did not show a significant difference between groups (t test, $P > 0.05$). The averaged time series duration was 538 ± 77 s for SNHL infants and 508 ± 111 s for TD infants, which did not show a significant difference between groups (t test, $P > 0.05$). Furthermore, we filtered out the first principal component through a principal components analysis (PCA) algorithm, to reduce the effect of global noise, which is generally associated with systemic fluctuations (e.g., arterial pulse, respiration, and cardiac pulsation) (*65*, *66*).

Calculating low-frequency hemoglobin signals

Last, we band-pass filtered the data between 0.009 and 0.08 Hz to remove low- frequency and high-frequency noise, such as cardiac noise and slow drift (*17*), and calculated the relative changes in the concentrations of oxyhemoglobin (HbO) and deoxyhemoglobin (HbR) on the basis of the modified Beer-Lambert law (*67*). We used the HbR signal to characterize topological characteristics of functional networks because it is the physiological basis of the blood oxygen level–dependent functional MRI signal (*68*, *69*) and has been shown to have higher test-retest reliability in an fNIRS-based brain network study (*70*).

Hemispheric network construction

To construct a brain network, two basic network elements must be determined: nodes and edges. For each hemisphere, measurement channels were considered to be nodes, and the functional connectivity between nodes were considered edges. Strength of edges was quantified by computing Pearson correlation coefficients for the time series between pairs of nodes. This strategy for hemisphere-specific network construction has been used in previous studies (*17*, *18*, *71*). Consistent with this and given the ambiguous biological basis for negative correlations in functional connectivity analyses, we set all negative correlations to zero and restricted our analysis to positive correlations. To improve the normality distribution of the correlations in the matrix, we converted correlation coefficients into z values via Fisher's r-to-z transformation. As in our previous studies (*17*, *18*), to ensure that the hemispheric networks have the same number of edges for each infant, we thresholded each correlation matrix into a weighted matrix with a fixed sparsity value, which was defined as the total number of edges in a network divided by the maximum possible number of edges. We chose sparsity (S) over a range of 0.1 to 0.5 with an interval of 0.01 for theoretical graph analysis of the hemispheric brain network, which would allow proper estimation of small-world network properties and minimization of the number of spurious edges in each network as indicated in previous studies (*72*–*74*).

Topological network measures

Network efficiency properties

Network efficiency properties were highly reliable (*70*, *75*) and have been frequently used to characterize the capability of parallel information processing within a brain network (*72*). We therefore focused on efficiency-related network properties in the current study in both SNHL and TD infant groups. Specifically, global network efficiency, local network efficiency, and nodal efficiency were computed within each hemisphere for each participant. For graph G with N nodes and M edges, the definitions for these parameters are described below.

Nodal efficiency

For arbitrary node i, nodal efficiency E_{nod} represents the capacity of node i to communicate with the other nodes of the network. The nodal efficiency was defined as the harmonic mean of the shortest path length between this node and all the other nodes in the network (*76*) and is calculated as follows

$$E_{\text{nod}}(i) = \frac{1}{N-1}\sum_{j\neq i\in G}\frac{1}{d(i,j)}$$

where $d(i,j)$ is the shortest path length between node i and node j.

Network global efficiency

The global efficiency E_{glob} of network G characterizes the global integration capacity of a network and is computed as the mean of the nodal efficiencies of all of the nodes of the network (*76*)

$$E_{\text{glob}}(G) = \frac{1}{N(N-1)}\sum\nolimits_{i\in G}\sum_{j\neq i\in G}\frac{1}{d_{ij}}$$

Network local efficiency

Local efficiency reflects the average communication ability of information flow within the local regions of the network. It also characterizes the average capability of a network to tolerate faults, i.e., how efficient the communication of the network is when any one node within the network is removed (*72*, *76*). The local efficiency of network G is calculated as follows

$$E_{\text{loc}}(G) = \frac{1}{N}\sum_{i\in G}E_{\text{glob}}(G_i)$$

Downloaded from https://www.science.org at University of California Merced on November 03, 2025

where $E_{glob}(G_i)$ is the global efficiency of G_i, the subgraph of the neighbors of node i. Generally, the brain network with higher local efficiency indicates the higher efficiency for the local information transfer.

These network properties were calculated using our in-house FC-NIRS package (*62*) (https://nitrc.org/projects/fcnirs), and the results reported in this study were based on a sparsity of 0.45.

Small-world efficiency analysis

Small-world properties are fundamental characteristics of human brain networks, which describes the capability of efficient global information integration and local information processing within network systems. Small-world network properties were originally proposed by Watts and Strogatz (*77*). Here, we used global network efficiency and local network efficiency to quantify the small-world properties of cortical networks in SNHL and TD infants, respectively. These network efficiency measures were compared separately to the corresponding indices derived from 1000 comparable random null networks. The random networks were generated by preserving the same numbers of nodes and edges and the same degree distribution as the brain network. Typically, a small-world network should meet the following criteria: Global efficiency in a real brain network is numerically approximate to that in a random network, and local efficiency in the brain network is larger than that in a random network. To investigate the small-world topology in SNHL infants and TD infants, we computed normalized E_{loc} and normalized E_{glob}, which were defined as the ratio of network efficiencies from real hemispheric networks to that from their matched random networks over a wide sparsity range (0.1~0.5).

Efficiency asymmetry calculation

To quantify the degree of asymmetry in efficiency measures between hemispheres, we calculated a commonly used AI, which was defined as follows

$$\mathrm{AI} = \frac{M_L - M_R}{M_L + M_R}$$

For network efficiencies, M_L and M_R represent the global or local efficiency of the entire left and right hemispheric network, respectively. For regional nodal efficiency, we divided these nodes into four regions (i.e., frontal, temporal, parietal, and occipital regions) according to the location information of the measurement channels (*17*), and M_L and M_R represent the mean nodal efficiency within different brain regions from the left and right hemispheric networks, respectively. Therefore, the AI in each cortical region was calculated as the averaged AI across these nodes within this region. The AI values range from −1 to 1, with a positive value of AI representing leftward asymmetry and a negative value of AI representing rightward asymmetry.

Statistical analysis

First, a GLM was adopted to evaluate age-related effects on hemispheric asymmetry (i.e., AI) of all network measures (i.e., global network efficiency, local network efficiency, and regional nodal efficiencies). The group (TD and SNHL), age, and group × age interaction was considered in this model as predictor variables, and gender was included as covariate. A significant group × age interaction suggested a difference in hemispheric asymmetry of network measure between two groups. To ascertain how the two groups differed in the developing trajectory of AI, a linear correlation analysis was conducted between the AI and age for each group, respectively.

Next, to investigate how the network efficiencies differ between these two hemispheres and differ between these two groups during the development, a new model with group, age, hemisphere, and all two-way and three-way interactions as predictor variables was used for analysis. If a significant group × age × hemisphere interaction was observed, a GLM that included hemisphere, age, hemisphere × age as predictor variables was used to explore how the two hemispheres differ in the development of network efficiencies in each group, another GLM that included group, age, group × age as predictor variables was used to understand how two groups differ in network efficiencies development within each hemisphere. After applying these two GLMs, we evaluated the correlations between age and network efficiencies in each hemisphere for each group to interpret the developmental trajectory details. Of note, multiple comparisons among groups, hemispheres and brain regions were considered by adopting the FDR correction, $P < 0.05$ after the correction was considered significant and gender was included as covariate for all GLMs.

Last, to examine how hearing loss severity affects the hemispheric asymmetry of network efficiency, we performed a GLM analysis with hearing loss severity (mild, moderate-to-severe, and profound), hemisphere, and their interaction as fixed effects, controlling for age and sex. Post hoc analyses were conducted to evaluate hemispheric differences in network efficiency within each subgroup. Multiple comparisons were corrected using the FDR method, with corrected P values < 0.05 considered statistically significant. In addition, we evaluated correlations between hearing loss severity (measured via ABR) and network efficiency metrics, including their lateralization indices, while adjusting for age and gender.

REFERENCES AND NOTES

1. A. R. T. Anastasio, A. Y. Yamamoto, E. T. Massuda, A. K. S. Manfredi, J. M. S. Cavalcante, B. C. P. Lopes, D. C. Aragon, S. Boppana, K. B. Fowler, W. J. Britt, M. M. Mussi-Pinhata, Comprehensive evaluation of risk factors for neonatal hearing loss in a large Brazilian cohort. *J. Perinatol.* **41**, 315–323 (2021).
2. C. T. Kraft, S. Malhotra, A. Boerst, M. C. Thorne, Risk indicators for congenital and delayed-onset hearing loss. *Otol. Neurotol.* **35**, 1839–1843 (2014).
3. X. Zhou, L. Wang, F. Jin, Y. Guo, Y. Zhou, X. Zhang, Y. Zhang, X. Ni, W. Li, H. Liu, The prevalence and risk factors for congenital hearing loss in neonates: A birth cohort study based on CHALLENGE study. *Int. J. Pediatr. Otorhinolaryngol.* **162**, 111308 (2022).
4. W. Yin, T. Li, Z. Wu, S.-C. Hung, D. Hu, Y. Gui, S. Cho, Y. Sun, M. A. Woodburn, L. Wang, G. Li, J. Piven, J. T. Elison, C. W. Wu, H. Zhu, J. R. Cohen, W. Lin, UNC/UMN Baby Connectome Project Consortium, Charting brain functional development from birth to 6 years of age. *Nat. Hum. Behav.* **9**, 1246–1259 (2025).
5. Q. Li, M. Xia, D. Zeng, Y. Xu, L. Sun, X. Liang, Z. Xu, T. Zhao, X. Liao, H. Yuan, Y. Liu, R. Huo, S. Li, Y. He, Development of segregation and integration of functional connectomes during the first 1,000 days. *Cell Rep.* **43**, 114168 (2024).
6. P. K. Kuhl, Brain mechanisms in early language acquisition. *Neuron* **67**, 713–727 (2010).
7. M. L. Hall, I.-M. Eigsti, H. Bortfeld, D. Lillo-Martin, Auditory deprivation does not impair executive function, but language deprivation might: Evidence from a parent-report measure in deaf native signing children. *J. Deaf Stud. Deaf Educ.* **22**, 9–21 (2017).
8. G. Dehaene-Lambertz, S. Dehaene, L. Hertz-Pannier, Functional neuroimaging of speech perception in infants. *Science* **298**, 2013–2015 (2002).
9. D. V. M. Bishop, Cerebral asymmetry and language development: Cause, correlate, or consequence? *Science* **340**, 1230531 (2013).
10. A. W. Toga, P. M. Thompson, Mapping brain asymmetry. *Nat. Rev. Neurosci.* **4**, 37–48 (2003).
11. O. A. Olulade, A. Seydell-Greenwald, C. E. Chambers, P. E. Turkeltaub, A. W. Dromerick, M. M. Berl, W. D. Gaillard, E. L. Newport, The neural basis of language development: Changes in lateralization over age. *Proc. Natl. Acad. Sci. U.S.A.* **117**, 23477–23483 (2020).
12. F. Dolcos, H. J. Rice, R. Cabeza, Hemispheric asymmetry and aging: Right hemisphere decline or asymmetry reduction. *Neurosci. Biobehav. Rev.* **26**, 819–825 (2002).
13. A. M. Chilosi, A. Comparini, P. Cristofani, M. Turi, S. Berrettini, F. Forli, G. Orlandi, A. Chiti, N. Giannini, P. Cipriani, G. Cioni, Cerebral lateralization for language in deaf children with cochlear implantation. *Brain Lang.* **129**, 1–6 (2014).
14. S. Jiwani, B. C. Papsin, K. A. Gordon, Early unilateral cochlear implantation promotes mature cortical asymmetries in adolescents who are deaf: Maturation with unilateral cochlear implants. *Hum. Brain Mapp.* **37**, 135–152 (2016).

Downloaded from https://www.science.org at University of California Merced on November 03, 2025

15. S. Telkemeyer, S. Rossi, S. P. Koch, T. Nierhaus, J. Steinbrink, D. Poeppel, H. Obrig, I. Wartenburger, Sensitivity of newborn auditory cortex to the temporal structure of sounds. *J. Neurosci.* **29**, 14726–14733 (2009).
16. J. Dubois, L. Hertz-Pannier, A. Cachia, J. F. Mangin, D. Le Bihan, G. Dehaene-Lambertz, Structural asymmetries in the infant language and sensori-motor networks. *Cereb. Cortex* **19**, 414–423 (2009).
17. G. Liu, E. Huo, H. Liu, G. Jia, Y. Zhi, Q. Dong, H. Niu, Development and emergence of functional network asymmetry in 3- to 9-month-old infants. *Cortex* **154**, 390–404 (2022).
18. L. Cai, Q. Dong, M. J. Wang, H. J. Niu, Functional near-infrared spectroscopy evidence for the development of topological asymmetry between hemispheric brain networks from childhood to adulthood. *Neurophotonics* **6**, 025005 (2019).
19. A. Kral, A. Sharma, Developmental neuroplasticity after cochlear implantation. *Trends Neurosci.* **35**, 111–122 (2012).
20. T. R. Barkat, D. B. Polley, T. K. Hensch, A critical period for auditory thalamocortical connectivity. *Nat. Neurosci.* **14**, 1189–1194 (2011).
21. S. Wang, B. Chen, Y. Yu, H. Yang, W. Cui, G. Fan, J. Li, Altered resting-state functional network connectivity in profound sensorineural hearing loss infants within an early sensitive period: A group ICA study. *Hum. Brain Mapp.* **42**, 4314–4326 (2021).
22. H. Zhao, Y. Wang, L. Cui, H. Wang, S. Liu, T. Liang, D. Liu, J. Qiu, L. Chen, Y. Sun, Sensorineural hearing loss and cognitive impairment: Three hypotheses. *Front. Aging Neurosci.* **16**, 1368232 (2024).
23. S. Wang, B. Chen, Y. Yu, H. Yang, W. Cui, J. Li, G. G. Fan, Alterations of structural and functional connectivity in profound sensorineural hearing loss infants within an early sensitive period: A combined DTI and fMRI study. *Dev. Cogn. Neurosci.* **38**, 100654 (2019).
24. S. Xia, T. Song, J. Che, Q. Li, C. Chai, M. Zheng, W. Shen, Altered brain functional activity in infants with congenital bilateral severe sensorineural hearing loss: A resting-state functional MRI study under sedation. *Neural Plast.* **2017**, 8986362 (2017).
25. D. Bavelier, D. P. Corina, H. J. Neville, Brain and Language. *Neuron* **21**, 275–278 (1998).
26. L. May, K. Byers-Heinlein, J. Gervain, J. F. Werker, Language and the newborn brain: Does prenatal language experience shape the neonate neural response to speech? *Front. Psychol.* **2**, 222 (2011).
27. Z. Hu, G. Liu, Q. Dong, H. Niu, Applications of resting-state fNIRS in the developing brain: A review from the connectome perspective. *Front. Neurosci.* **14**, 476 (2020).
28. H. Niu, Y. He, Resting-state functional brain connectivity: Lessons from functional near-infrared spectroscopy. *Neuroscientist* **20**, 173–188 (2014).
29. L. Cai, Q. Dong, H. Niu, The development of functional network organization in early childhood and early adolescence: A resting-state fNIRS study. *Dev. Cogn. Neurosci.* **30**, 223–235 (2018).
30. K. Zeng, J. Kang, G. Ouyang, J. Li, J. Han, Y. Wang, E. M. Sokhadze, M. F. Casanova, X. Li, Disrupted brain network in children with autism spectrum disorder. *Sci. Rep.* **7**, 16253 (2017).
31. J. H. Ko, P. G. Spetsieris, D. Eidelberg, Network structure and function in Parkinson's disease. *Cereb. Cortex* **28**, 4121–4135 (2018).
32. X. Zhao, Y. Liu, X. Wang, B. Liu, Q. Xi, Q. Guo, H. Jiang, T. Jiang, P. Wang, Disrupted small-world brain networks in moderate Alzheimer's Disease: A resting-state fMRI study. *PLOS ONE* **7**, e33540 (2012).
33. W. Li, J. Li, J. Wang, P. Zhou, Z. Wang, J. Xian, H. He, Functional reorganizations of brain network in prelingually deaf adolescents. *Neural Plast.* **2016**, 9849087 (2016).
34. P. Adibpour, J. Lebenberg, C. Kabdebon, G. Dehaene-Lambertz, J. Dubois, Anatomo-functional correlates of auditory development in infancy. *Dev. Cogn. Neurosci.* **42**, 100752 (2020).
35. J. Brauer, J. Neumann, A. D. Friederici, Temporal dynamics of perisylvian activation during language processing in children and adults. *Neuroimage* **41**, 1484–1492 (2008).
36. J. S. Allen, K. Emmorey, J. Bruss, H. Damasio, Neuroanatomical differences in visual, motor, and language cortices between congenitally deaf signers, hearing signers, and hearing non-signers. *Front. Neuroanat.* **7**, 26 (2013).
37. T. Twomey, D. Waters, C. J. Price, S. Evans, M. MacSweeney, How auditory experience differentially influences the function of left and right superior temporal cortices. *J. Neurosci.* **37**, 9564–9573 (2017).
38. H. Payne, E. Gutierrez-Sigut, B. Woll, M. MacSweeney, Cerebral lateralisation during signed and spoken language production in children born deaf. *Dev. Cogn. Neurosci.* **36**, 100619 (2019).
39. S. Ocklenburg, Z. V. Guo, Cross-hemispheric communication: Insights on lateralized brain functions. *Neuron* **112**, 1222–1234 (2024).
40. M. Kinsbourne, "Development of cerebral lateralization in children" in *Handbook of Clinical Child Neuropsychology*, C. R. Reynolds, E. Fletcher-Janzen, Eds. (Springer US, 2009), pp. 47–66.
41. N. Paquette, M. Lassonde, P. Vannasing, J. Tremblay, B. González-Frankenberger, O. Florea, R. Béland, F. Lepore, A. Gallagher, Developmental patterns of expressive language hemispheric lateralization in children, adolescents and adults using functional near-infrared spectroscopy. *Neuropsychologia* **68**, 117–125 (2015).
42. C. J. Wild, A. C. Linke, L. Zubiaurre-Elorza, C. Herzmann, H. Duffy, V. K. Han, D. S. C. Lee, R. Cusack, Adult-like processing of naturalistic sounds in auditory cortex by 3- and 9-month old infants. *Neuroimage* **157**, 623–634 (2017).
43. T. Imada, Y. Zhang, M. Cheour, S. Taulu, A. Ahonen, P. K. Kuhl, Infant speech perception activates Broca's area: A developmental magnetoencephalography study. *Neuroreport* **17**, 957–962 (2006).
44. Y. Minagawa-Kawai, A. Cristià, E. Dupoux, Cerebral lateralization and early speech acquisition: A developmental scenario. *Dev. Cogn. Neurosci.* **1**, 217–232 (2011).
45. J. Zhu, J. Cui, G. Cao, J. Ji, X. Chang, C. Zhang, Y. Liu, Brain functional alterations in long-term unilateral hearing impairment. *Acad. Radiol.* **27**, 1085–1092 (2020).
46. D. R. Moore, J. T. Devlin, J. Raley, E. Tunbridge, K. Lanary, A. Floyer-Lea, C. Narain, I. Cohen, P. Jezzard, M. J. Burton, P. M. Matthews, "Effects of long term unilateral hearing loss on the lateralization of fMRI measured activation in human auditory cortex" in *Plasticity and Signal Representation in the Auditory System*, J. Syka, M. M. Merzenich, Eds. (Springer US, 2005), pp. 335–346.
47. S. J. Gotts, H. J. Jo, G. L. Wallace, Z. S. Saad, R. W. Cox, A. Martin, Two distinct forms of functional lateralization in the human brain. *Proc. Natl. Acad. Sci. U.S.A.* **110**, E3435–E3444 (2013).
48. J. Tan, Q.-M. Hou, F. Zhang, X. Duan, Y.-L. Zhang, Y.-J. Lee, H. Yan, Brain networks in newborns and infants with and without sensorineural hearing loss: A functional near-infrared spectroscopy study. *World J. Psychiatry* **14**, 1547–1557 (2024).
49. E. Bullmore, O. Sporns, Complex brain networks: Graph theoretical analysis of structural and functional systems. *Nat. Rev. Neurosci.* **10**, 186–198 (2009).
50. C. R. Lyness, B. Woll, R. Campbell, V. Cardin, How does visual language affect crossmodal plasticity and cochlear implant success? *Neurosci. Biobehav. Rev.* **37**, 2621–2630 (2013).
51. S. L. Pallas, Intrinsic and extrinsic factors that shape neocortical specification. *Trends Neurosci.* **24**, 417–423 (2001).
52. A. Sharma, M. F. Dorman, A. Kral, The influence of a sensitive period on central auditory development in children with unilateral and bilateral cochlear implants. *Hear. Res.* **203**, 134–143 (2005).
53. A. Calcus, O. Tuomainen, A. Campos, S. Rosen, L. F. Halliday, Functional brain alterations following mild-to-moderate sensorineural hearing loss in children. *Elife* **8**, e46965 (2019).
54. A. D. Friederici, The brain basis of language processing: From structure to function. *Physiol. Rev.* **91**, 1357–1392 (2011).
55. K. A. Gordon, D. D. E. Wong, B. C. Papsin, Bilateral input protects the cortex from unilaterally-driven reorganization in children who are deaf. *Brain* **136**, 1609–1625 (2013).
56. S. Salandy, R. Rai, S. Gutierrez, B. Ishak, R. S. Tubbs, Neurological examination of the infant: A comprehensive review. *Clin. Anat.* **32**, 770–777 (2019).
57. Joint Committee on Infant Hearing, Year 2019 Position Statement: Principles and Guidelines for Early Hearing Detection and Intervention Programs (2019); https://infanthearing.org/nhstc/docs/Year%202019%20JCIH%20Position%20Statement.pdf.
58. I. Kovelman, M. H. Shalinsky, M. S. Berens, L.-A. Petitto, Shining new light on the brain's "bilingual signature": A functional near infrared spectroscopy investigation of semantic processing. *Neuroimage* **39**, 1457–1471 (2008).
59. S. Sasai, F. Homae, H. Watanabe, A. T. Sasaki, H. C. Tanabe, N. Sadato, G. Taga, A NIRS–fMRI study of resting state network. *Neuroimage* **63**, 179–193 (2012).
60. J. Ye, S. Tak, K. Jang, J. Jung, J. Jang, NIRS-SPM: Statistical parametric mapping for near-infrared spectroscopy. *Neuroimage* **44**, 428–447 (2009).
61. N. Tzourio-Mazoyer, B. Landeau, D. Papathanassiou, F. Crivello, O. Etard, N. Delcroix, B. Mazoyer, M. Joliot, Automated anatomical labeling of activations in SPM using a macroscopic anatomical parcellation of the MNI MRI single-subject brain. *Neuroimage* **15**, 273–289 (2002).
62. J. Xu, X. Liu, J. Zhang, Z. Li, X. Wang, F. Fang, H. Niu, FC-NIRS: A functional connectivity analysis tool for near-infrared spectroscopy data. *Biomed. Res. Int.* **2015**, 248724 (2015).
63. F. Scholkmann, S. Spichtig, T. Muehlemann, M. Wolf, How to detect and reduce movement artifacts in near-infrared imaging using moving standard deviation and spline interpolation. *Physiol. Meas.* **31**, 649–662 (2010).
64. S. Geng, X. Liu, B. B. Biswal, H. Niu, Effect of resting-state fNIRS scanning duration on functional brain connectivity and graph theory metrics of brain network. *Front. Neurosci.* **11**, 392 (2017).
65. A. Abdalmalak, S. L. Novi, K. Kazazian, L. Norton, T. Benaglia, M. Slessarev, D. B. Debicki, K. St Lawrence, R. C. Mesquita, A. M. Owen, Effects of systemic physiology on mapping resting-state networks using functional near-infrared spectroscopy. *Front. Neurosci.* **16**, 803297 (2022).
66. M. A. Franceschini, D. K. Joseph, T. J. Huppert, S. G. Diamond, D. A. Boas, Diffuse optical imaging of the whole head. *J. Biomed. Opt.* **11**, 054007 (2006).
67. L. Kocsis, P. Herman, A. Eke, The modified Beer–Lambert law revisited. *Phys. Med. Biol.* **51**, N91–N98 (2006).
68. R. B. Buxton, E. C. Wong, L. R. Frank, Dynamics of blood flow and oxygenation changes during brain activation: The balloon model. *Magn. Reson. Med.* **39**, 855–864 (1998).
69. S. Ogawa, R. S. Menon, D. W. Tank, S. G. Kim, H. Merkle, J. M. Ellermann, K. Ugurbil, Functional brain mapping by blood oxygenation level-dependent contrast magnetic

Downloaded from https://www.science.org at University of California Merced on November 03, 2025

resonance imaging. A comparison of signal characteristics with a biophysical model. *Biophys. J.* **64**, 803–812 (1993).
70. H. Niu, Z. Li, X. Liao, J. Wang, T. Zhao, N. Shu, X. Zhao, Y. He, Test-retest reliability of graph metrics in functional brain networks: A resting-state fNIRS study. *PLOS ONE* **8**, e72425 (2013).
71. Y. Iturria-Medina, A. Pérez Fernández, D. M. Morris, E. J. Canales-Rodríguez, H. A. Haroon, L. García Pentón, M. Augath, L. Galán García, N. Logothetis, G. J. M. Parker, L. Melie-García, Brain hemispheric structural efficiency and interconnectivity rightward asymmetry in human and nonhuman primates. *Cereb. Cortex* **21**, 56–67 (2011).
72. S. Achard, E. Bullmore, Efficiency and cost of economical brain functional networks. *PLOS Comput. Biol.* **3**, e17 (2007).
73. H. Niu, J. Wang, T. Zhao, N. Shu, Y. He, Revealing topological organization of human brain functional networks with resting-state functional near infrared spectroscopy. *PLOS ONE* **7**, e45771 (2012).
74. W. Yin, M.-H. Chen, S.-C. Hung, K. R. Baluyot, T. Li, W. Lin, Brain functional development separates into three distinct time periods in the first two years of life. *Neuroimage* **189**, 715–726 (2019).
75. M. Wang, Z. Yuan, H. Niu, Reliability evaluation on weighted graph metrics of fNIRS brain networks. *Quant. Imaging Med. Surg.* **9**, 832–841 (2019).
76. V. Latora, M. Marchiori, Efficient behavior of small-world networks. *Phys. Rev. Lett.* **87**, 198701 (2001).
77. D. J. Watts, S. H. Strogatz, Collective dynamics of 'small-world' networks. *Nature* **393**, 440–442 (1998).

Acknowledgments
Funding: This work was supported by the STI 2030—Major Projects grant 2021ZD0200500 and National Key R&D Program of China grant 2023YFF1203504. **Author contributions:** Conceptualization: H.N., H.L., and Q.D. Methodology: G.L., Z.H., E.H., and H.N. Visualization: G.L., Z.H., and E.H. Investigation: G.L., X.Z., and Y.L. Supervision: H.N., H.L., and H.B. Writing—original draft: G.L., X.Z., Z.H., E.H., Y.L., H.N., and H.L. Writing—review and editing: Z.H., E.H., C.C., H.B., and H.N. **Competing interests:** The authors declare that they have no competing interests. **Data and materials availability:** All data needed to evaluate the conclusions in the paper are present in the paper and on Dryad: https://doi.org/10.5061/dryad.8kprr4z0t.

Submitted 18 March 2025
Accepted 15 September 2025
Published 15 October 2025
10.1126/sciadv.adx1327

Downloaded from https://www.science.org at University of California Merced on November 03, 2025